

# Evolutionary Dynamics in an Individual Spatial and a Mean Field Differential Equation Host-Pathogen Model

William B. Zhang  
Mathematics Undergraduate Thesis  
Department of Mathematics, Duke University  
Durham, North Carolina 27708 USA

January 29, 2014

# Acknowledgements

First and foremost, I would like to thank my advisor, Rick Durrett. Thank you for adopting me as a student, guiding me through this project, and always being available to talk through the obstacles that came up. Your insights and suggestions made this project manageable and helped me move past many potential roadblocks. This thesis would not have been possible without you. Thank you.

I would also like to thank Jianfeng Lu for helpful comments on earlier drafts and for interesting discussions regarding the project, David Kraines for organizing the mathematics major senior talks and other events, and the entire mathematics community at Duke University for a wonderful four years!



## **Abstract**

We examine a host-pathogen model in which three types of species exist: empty sites, healthy hosts, and infected hosts. In this model six different transitions can occur: empty sites can be colonized by healthy hosts, healthy hosts can be infected, and infected hosts can either recover or die. We implement this general model in both a spatial context with discrete time and in a homogeneously mixing model in continuous time. We then explore evolution for pairs of parameters, calculating viable regions in the ODE model and evolutionary vector fields in both models. Our results show that results from the spatial model do not always converge to our ODE model results, that stochasticity in the spatial evolutionary vector field can be used as a measure of the magnitude of evolutionary pressure and as an indicator of non-viable parameters, and that the evolutionary pressures on different parameters are not necessarily independent. For example, a lower transmissibility greatly lowers the magnitude of evolutionary pressure for all parameters associated with transitions from infected hosts.

# Contents

<b>1</b>	<b>Introduction</b>	<b>3</b>
1.1	Motivation for Host-Pathogen Models . . . . .	3
1.2	The General Host-Pathogen Model . . . . .	3
1.3	Motivation for Spatial Models . . . . .	4
1.4	The Individual-Based Spatial Model . . . . .	5
1.4.1	Square Lattice and Discrete Time . . . . .	5
1.4.2	Probabilities of Events . . . . .	6
1.5	The Mean-Field Differential Equation Model . . . . .	8
1.5.1	Differences from the Spatial Model . . . . .	9
1.5.2	The System of Equations . . . . .	9
1.5.3	The Meaning of the Parameters . . . . .	9
1.6	Limitations and Assumptions of This Formulation . . . . .	10
<b>2</b>	<b>Methods</b>	<b>11</b>
2.1	Python Simulations . . . . .	11
2.1.1	Pathogen Spatial Evolution Simulations . . . . .	11
2.1.2	Host Spatial Evolution Simulation Procedure . . . . .	11
2.1.3	Host Differential Equation Viability Simulations . . . . .	12
2.1.4	Host Differential Equation Evolutionary Pressure . . . . .	12
<b>3</b>	<b>Results</b>	<b>13</b>
3.1	Evolution on the Pathogen Side . . . . .	13
3.2	Pathogen $\mu$ - $\beta$ Evolution . . . . .	14
3.2.1	Viable Region . . . . .	14
3.2.2	Fitness . . . . .	15
3.2.3	Direction of Evolution . . . . .	17
3.2.4	Spatial Evolution Simulation . . . . .	18
3.3	Pathogen $\gamma$ - $\beta$ Evolution . . . . .	19
3.3.1	Viable Region . . . . .	19
3.3.2	Fitness . . . . .	20
3.3.3	Direction of Evolution . . . . .	21
3.3.4	Spatial Evolution Simulation . . . . .	22
3.4	Pathogen $\mu$ - $\gamma$ Evolution . . . . .	23
3.4.1	Viable Region . . . . .	23
3.4.2	Fitness . . . . .	24

3.4.3	Direction of Evolution . . . . .	25
3.4.4	Spatial Evolution Simulation . . . . .	26
3.5	Evolution on the Host Side . . . . .	27
3.5.1	Preliminary Analysis for $\alpha$ - $\beta$ Evolution . . . . .	27
3.5.2	Approach to Host Side Evolution . . . . .	29
3.6	Host $\alpha$ - $\beta$ Evolution . . . . .	30
3.7	Host $\alpha$ - $\gamma$ Evolution . . . . .	31
3.8	Host $\alpha$ - $\mu$ Evolution . . . . .	32
3.9	Host $\beta$ - $\gamma$ Evolution . . . . .	33
3.10	Host $\beta$ - $\mu$ Evolution . . . . .	34
3.11	Host $\gamma$ - $\mu$ Evolution . . . . .	35
<b>4</b>	<b>Discussion</b>	<b>36</b>
4.1	Direction of Evolutionary Pressure . . . . .	36
4.1.1	$\beta$ -Dependence of Parameters Associated with Infected Hosts . . . . .	36
4.2	Stochasticity in Spatial Model . . . . .	37
4.2.1	As a Measure of Evolutionary Pressure . . . . .	37
4.2.2	High Stochasticity in Non-Viable Region . . . . .	37

# Chapter 1

## Introduction

### 1.1 Motivation for Host-Pathogen Models

With the advent of air travel and steel skyscrapers, human populations have enjoyed increased mobility and have achieved high population densities in urban centers. As a result, the potential impact of infectious diseases and parasites has significantly increased, and the study of pathogens has become a public health priority [7]. In particular, we are concerned about the emergence of new highly virulent species that can spread rapidly [5]. To better understand the evolutionary mechanisms which produce new pathogen strains, we can focus on a limited group of species and a limited number of transitions between them. We then introduce parameters for the rates of these transitions and study the resulting trajectories as these parameters are allowed to evolve.

### 1.2 The General Host-Pathogen Model

Our general host-pathogen model is one of many possible formulations [4]. In our model, an uninfected host is able to reproduce at a rate  $\alpha$ , and can be infected by a parasite at a rate  $\beta$ . Infected hosts can die at a rate  $\mu$ , leaving a vacancy, or recover to an uninfected state at rate  $\gamma$ . Uninfected hosts can never die, infected hosts can never reproduce, and pathogens do not exist outside of infected hosts. These transitions are shown in figure 1.1, with corresponding parameter names for the spatial model given in parentheses.

We now notice that we have three types of species in simulation: vacant sites, uninfected hosts, and infected hosts (or pathogens). We will focus on uninfected and infected hosts, since the densities of all three types of species sum to 1. We see that there is one parameter associated with the transition between healthy hosts and vacant sites,  $\alpha$ , two associated with the transition between healthy hosts and infected hosts,  $\beta$  and  $\gamma$ , and one parameter associated with the transition between infected hosts and empty sites,  $\mu$ . Note that since an infected host consists of a pathogen of type  $j$  infecting a host of type  $i$ , the rates of its transitions can depend on both the type of healthy host from which it was derived, and the type of pathogen infecting it. For example, in a system with pathogens A, B, and C, and hosts 1, 2, and 3, host 2 infected with pathogen B may die faster than host 2 infected with pathogen A (virulence as a pathogen trait), but host 2 infected with pathogen B may also

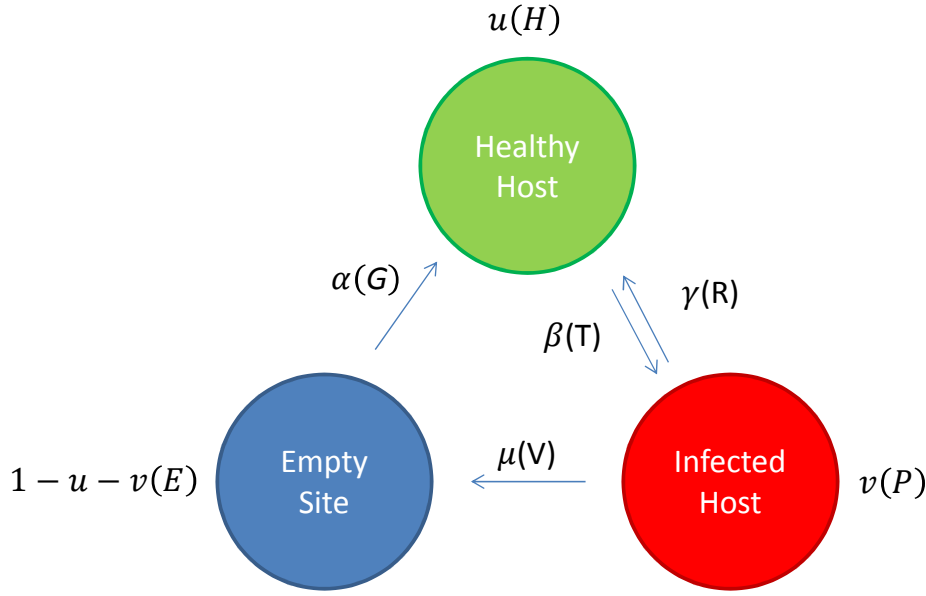


Figure 1.1: A schematic of the possible states that exist in our system, the allowed transitions, and the parameters governing their rates.

die faster than host 1 infected with pathogen B (virulence as a host trait). In a system with  $n$  hosts and  $m$  pathogens, we can think of  $\alpha$  as an  $n$ -dimensional vector, and  $\beta$ ,  $\gamma$ , and  $\mu$  as  $n \times m$  matrices.

In some sense, then, we have three host-side parameters and four pathogen-side parameters, since  $\beta$ ,  $\gamma$ , and  $\mu$  are dependent on both the host and pathogen. The simplest case is pathogen evolution. We can begin with a single host and single pathogen, then introduce a second pathogen with different parameters, and allow the two to compete. For host evolution, we have three biological species present: two competing types of host and one type of pathogen. But we need four species in the system, since each healthy host has a distinct infected counterpart. If we go beyond this, and allow both the host and pathogen to evolve, we would have at least four biological species (two pathogens and two hosts), resulting in six species in simulation (two healthy hosts, and four types of infected hosts). Things become unmanageable very quickly. For this reason, we limit the scope of this project to pairs of host-side parameters and pairs of pathogen-side parameters.

### 1.3 Motivation for Spatial Models

An appropriate balance between simplicity and realism is critical to building an effective model. If a model favors either disproportionately, its utility will be drastically diminished. If simplicity is sacrificed, it will be difficult to interpret one's results and to draw general conclusions; but without realism, results will not be applicable to the corresponding real-world systems.

One traditional simplification assumes homogeneous mixing — every individual in the

system is in contact with every other individual<sup>1</sup> — in models for spatially extended systems. However, this has recently come under examination. Researchers have come to understand that in spatially extended systems, individuals are primarily influenced by their local environment. Non-equilibrium fluctuations and stochastically generated spatial inhomogeneities can influence their local environment and generate stable long-term behavior.

Intermediate models, such as reaction-diffusion systems [6] and ‘patch’ models [2] have partially accounted for these spatial effects by assuming local mixing, with dispersion between local neighborhoods. While these models represent improvements over mean-field models with homogeneous mixing, exact, agent-based models, can more fully capture the effects of discreteness, stochasticity, and space.

In this paper, we examine a host-pathogen system from both a spatial perspective and using a traditional mean-field ordinary differential equation model. The precise formulations of both our spatial and differential equation models are drawn from Rand, Keeling, and Wilson’s 1995 study [3], and have four groups of parameters — host growth, transmissibility, virulence, and recovery. Here, we comprehensively explore the dynamics that arise when pairs of parameters are allowed to evolve, and contrast them across the two models.

## 1.4 The Individual-Based Spatial Model

Here, we consider a system with  $a$  species of hosts and  $b$  species of pathogens<sup>2</sup>, resulting in  $ab$  different types of infected hosts, and  $a + ab + 1$  total species in simulation. In this system we have four essential groups of parameters: (i) the growth rates associated with each host type,  $g_i$ <sup>3</sup> (analogous to the  $\alpha$  in the general system), (ii) the virulence, or death rate, of pathogen type  $j$  infecting host type  $i$ ,  $v_{ij}$  (analogous to  $\mu$ ), (iii) the transmissibility of pathogen type  $j$  to host type  $i$ ,  $\tau_{ij}$  (analogous to  $\beta$ ), and (iv) the recovery rate of host type  $i$  infected with pathogen type  $j$ ,  $r_{ij}$  (analogous to  $\gamma$ ).

### 1.4.1 Square Lattice and Discrete Time

In the individual-based spatial model, the environment is an  $L \times L$  square lattice consisting of the points in (1.4.1).

$$\vec{x} = \begin{bmatrix} x_1 \\ x_2 \end{bmatrix} \in \mathbb{Z}^2 \text{ where } 0 \leq x_1, x_2 < L \quad (1.4.1)$$

We also denote the state of the system at a given time  $t$  as  $\zeta_t$ , where  $\zeta_t(\vec{x})$  gives the state of site  $\vec{x}$  at time  $t$ .

---

<sup>1</sup>This contrasts with spatial models, in which individuals are only in contact with others in a local neighborhood.

<sup>2</sup>When we speak about the ordinary differential equation model, we will use the same symbols as we do for the general model, but for clarity we will use different, but analogous, symbols and indices for the spatial model.

<sup>3</sup>We will generally use  $i$  to refer to the index of a particular host strain, and  $j$  to refer to the index of a particular pathogen strain.

Each site in the lattice can either be empty ( $\zeta_t(\vec{x}) = E$ ), contain a healthy host of type  $i$  ( $\zeta_t(\vec{x}) = H_i$ ), or contain an infected host of type  $ij$  ( $\zeta_t(\vec{x}) = P_{ij}$ , created from a healthy host of type  $i$  infected by a pathogen of type  $j$ ). Our model uses discrete time, so we have time steps after which the lattice is updated. In addition, we update our lattice synchronously, so that at every time step, every site in the lattice is updated (as opposed to asynchronous updating, in which only certain sites are updated each time step).

In this model, the state of a site at time  $t+1$ ,  $\zeta_{t+1}(\vec{x})$  is affected by the state of sites in its von Neumann neighborhood,  $N(\vec{x})$  at time  $t$ , which is defined in (1.4.2).

$$N(\vec{x}) = \begin{bmatrix} x_1 - 1 \\ x_2 \end{bmatrix}, \begin{bmatrix} x_1 + 1 \\ x_2 \end{bmatrix}, \begin{bmatrix} x_1 \\ x_2 - 1 \end{bmatrix}, \begin{bmatrix} x_1 \\ x_2 + 1 \end{bmatrix} \quad (1.4.2)$$

This neighborhood basically includes all sites directly adjacent to the site of interest.

### 1.4.2 Probabilities of Events

The following table of probabilities is adapted from Table 1 in [3]<sup>4</sup>

$\zeta_t(\vec{x})$	$P(\zeta_{t+1}(\vec{x}) = E)$	$P(\zeta_{t+1}(\vec{x}) = H_i)$	$P(\zeta_{t+1}(\vec{x}) = P_{ij})$
$E$	$\prod_{k=1}^a (1 - g_k)^{n_k}$	$\frac{\left[1 - \prod_{k=1}^a (1 - g_k)^{n_k}\right] [1 - (1 - g_i)^{n_i}]}{\sum_{k=1}^a [1 - (1 - g_k)^{n_k}]}$	0
$H_i$	0	$\prod_{k=1}^b (1 - \tau_{ik})^{m_k}$	$\frac{\left[1 - \prod_{k=1}^b (1 - \tau_{ik})^{m_k}\right] [1 - (1 - \tau_{ij})^{m_j}]}{\sum_{k=1}^b [1 - (1 - \tau_{ik})^{m_k}]}$
$P_{ij}$	$v_{ij}$	$r_{ij}$	$1 - v_{ij} - r_{ij}$

Table 1.1: A table of the probability distribution of the future states of a site, given a neighborhood  $N(\vec{x})$  at time  $t$  containing  $n_i$  members of host type  $H_i$  and  $m_j$  individuals infected with by pathogen  $j$ .

Now, let's try to derive these equations from first principles. Suppose that (i)  $g_i$  is the probability of a particular host of type  $i$  in the neighborhood of an empty site colonizing that site after one time step in the absence of competition from other hosts, (ii)  $v_{ij}$  is the probability of a particular host of type  $i$  infected with a pathogen of type  $j$  dying after one time step, (iii)  $\tau_{ij}$  is the probability of a host of type  $i$  being infected by a particular pathogen of type  $j$  in its neighborhood after one time step in the absence of competition from other pathogens, and (iv)  $r_{ij}$  is the probability of a type  $i$  host infected with pathogen type  $j$  recovering to a healthy host after one time step.

Let's begin with the case when  $\zeta_t(\vec{x}) = E$ . We know that two things can happen to an empty site: (i) it can remain an empty site, or (ii) it can be colonized by a species of host.

<sup>4</sup>There is a typographical error in the original table in [3] for the entry for  $P(\zeta_{t+1}(\vec{x}) = P_{ij})$  when  $\zeta_t(\vec{x}) = H_i$ . The  $n_j$ 's in the original should be  $m_j$ 's, and the  $\Sigma$  in the denominator should have a  $j$  subscript. Further, the equation for  $P(\zeta_{t+1}(\vec{x}) = P_{ij})$  when  $P(\zeta_t(\vec{x}) = P_{ij})$  has been modified from [3], since in the original the probabilities for the case  $P(\zeta_t(\vec{x}) = P_{ij})$  do not sum to one when  $v_{ij}, r_{ij} \neq 0$ .

So to start, we know that  $P(\zeta_{t+1}(\vec{x}) = P_{ij}) = 0$  in this case. Further, we realize that all that we need for this site to remain empty is for all of the hosts in its neighborhood to fail to colonize it. Since there is no competition in this case (all hosts fail), the probability that a particular host of type  $k$  fails to colonize our empty site (in the absence of competition) is  $1 - g_k$ , so the probability that no host of type  $k$  colonizes our empty site is  $(1 - g_k)^{n_k}$ , and the probability of no host of any type colonizing our empty site — and our site remaining empty — is

$$\prod_{k=1}^a (1 - g_k)^{n_k}. \quad (1.4.3)$$

On the other hand, the probability of our empty site being colonized by a host of type  $i$  is a bit more difficult. The probability of our site being colonized by any host at all is given by

$$1 - \prod_{k=1}^a (1 - g_k)^{n_k}. \quad (1.4.4)$$

As we saw before, the probability of a host of type  $k$  fails to colonize our empty site (in the absence of competition) is  $(1 - g_k)^{n_k}$ . Assuming that the probability of a type of host colonizing an empty site with competition is proportional to the probability that it fails to colonize that site in the absence of competition subtracted from 1, we have that the probability of a host of type  $i$  successfully colonizing our site, given that some host successfully colonizes that site, is proportional to  $1 - (1 - g_i)^{n_i}$ . We can normalize this expression by dividing by,

$$\sum_{k=1}^a [1 - (1 - g_k)^{n_k}], \quad (1.4.5)$$

the sum of all of these “proportional terms”. So, the probability of a host of type  $i$  successfully colonizing our empty site, given that some host successfully colonizes our empty site, is given by

$$\frac{[1 - (1 - g_i)^{n_i}]}{\sum_{k=1}^a [1 - (1 - g_k)^{n_k}]}. \quad (1.4.6)$$

Now by Bayes’ Theorem [1], we know that the probability of a host of type  $i$  successfully colonizing our site is indeed

$$\frac{\left[1 - \prod_{k=1}^a (1 - g_k)^{n_k}\right] [1 - (1 - g_i)^{n_i}]}{\sum_{k=1}^a [1 - (1 - g_k)^{n_k}]}. \quad (1.4.7)$$

Next, let’s consider the case in which we have  $\zeta_t(\vec{x}) = H_i$ . We know that when a site contains a host of type  $i$ , at the next time step it can either remain a host of type  $i$  or become



infected with a pathogen. It is not possible for a host to directly transition to an empty cell. Therefore, we know that  $P(\zeta_{t+1}(\vec{x}) = E) = 0$ . Next, we note that the probability of a host site remaining a host is the same as the probability of all pathogens in its neighborhood failing to colonize it. Similar to an empty site remaining empty, since there is no competition in this case (all pathogens fail), we have that the probability that a particular pathogen of type  $k$  fails to colonize our host is  $1 - \tau_k$ , so the probability that no host of type  $k$  colonizes our empty site is  $(1 - \tau_k)^{m_k}$ , and the probability of no host of any type colonizing our empty site — and our site remaining empty — is

$$\prod_{k=1}^b (1 - \tau_k)^{m_k}. \quad (1.4.8)$$

The other possible outcome when  $\zeta_t(\vec{x}) = H_i$  is that some pathogen successfully infects our host,  $\zeta_{t+1}(\vec{x}) = P_{ij}$ . To find the probabilities for each particular type of pathogen, we begin by considering the probability that some pathogen infects our host. This value,

$$1 - \prod_{k=1}^b (1 - \tau_{ik})^{m_k}, \quad (1.4.9)$$

is simply the probability that no pathogen infects our host subtracted from one. Further, if we assume that the probability that a particular type of pathogen infects our host is proportional to the probability that it fails to infect, subtracted from one. So we have that  $P(\zeta_{t+1}(\vec{x}) = P_{ij}) \propto 1 - (1 - \tau_{ij})^{m_j}$ . We can normalize this expression by dividing by the sum of all of these proportional terms and multiplying by the overall probability that any pathogen infects the host. This yields the expected expression,

$$\frac{\left[1 - \prod_{k=1}^b (1 - \tau_{ik})^{m_k}\right] [1 - (1 - \tau_{ij})^{m_j}]}{\sum_{k=1}^b [1 - (1 - \tau_{ik})^{m_k}]}. \quad (1.4.10)$$

Lastly, we consider the case when  $P(\zeta_t(\vec{x}) = P_{ij})$ . While hosts compete to colonize empty sites and pathogens compete to infect hosts, no species compete over the fate of infected hosts. For this reason, the equations governing the distribution of outcomes for infected hosts are simpler. The probability of an infected host of type  $ij$  (host  $i$  and pathogen  $j$ ) dying and leaving an empty site is simply the virulence,  $v_{ij}$ , while the probability of recovering to its healthy state is simply the recovery rate,  $r_{ij}$ , and the probability of our infected host remaining infected is simply the probabilities of the other cases subtracted from one,  $1 - v_{ij} - r_{ij}$ .

## 1.5 The Mean-Field Differential Equation Model

In the differential equation model, just as in the spatial model, we consider a system with  $a$  species of hosts and  $b$  species of pathogens, resulting in  $ab$  different types of infected hosts, and  $a+ab+1$  total species in simulation. Analogously, in this system we also have four groups

of parameters: (i) the growth rates associated with each host type,  $\alpha_i$ , (ii) the virulence, or death rate, of pathogen type  $j$  infecting host type  $i$ ,  $\mu_{ij}$ , (iii) the transmissibility of pathogen type  $j$  to host type  $i$ ,  $\beta_{ij}$ , and (iv) the recovery rate of host type  $i$  infected with pathogen type  $j$ ,  $\gamma_{ij}$ .

### 1.5.1 Differences from the Spatial Model

There are several important differences between the differential equation model and the previously described spatial model. In the ODE all species in the system are in contact with each other, and may interact at any point — there is no spatial isolation. In addition, since this model uses a continuum of possible quantities of each species, it cannot capture the effects of discreteness and stochasticity. Finally, while the spatial model was run in discrete time, effectively limiting the rate at which events can occur (only one event per site per time step), the differential equation model is in continuous time, so the parameters that represented probabilities in the spatial model are now direct rates.

### 1.5.2 The System of Equations

Let the proportion of hosts of type  $i$  in our system be given by  $u_i$  and the proportion of infected hosts of type  $ij$  (from host  $i$  and pathogen  $j$ ) be given by  $v_{ij}$ . For the simplest system, in which there is only one type of host and one type of pathogen (and therefore only one type of infected host), we can discard all subscripts, and see that equations (1.5.1) and (1.5.2) describe the time-evolution of the host and pathogen populations.

$$\frac{du}{dt} = \alpha u (1 - u - v) - \beta uv + \gamma v \quad (1.5.1)$$

$$\frac{dv}{dt} = \beta uv - (\gamma + \mu) v \quad (1.5.2)$$

### 1.5.3 The Meaning of the Parameters

As mentioned earlier, the parameters in the differential equation model have slightly different interpretations than the analogous ones in the spatial model. Since the differential equation model is in continuous time, the interpretations of the parameters are much more straightforward.<sup>5</sup> While the spatial model parameters represented probabilities, they only did so with the caveat that there were no competing species in the von Neumann neighborhood. When competition is present, the expressions need to be normalized to be interpreted as probabilities. In other words, competing species in the system will directly affect the behavior of each species at each time point, as evidenced by the expressions for  $\zeta_{t+1}(\vec{x}) = H_i$  when  $\zeta_t(\vec{x}) = E$  and  $\zeta_{t+1}(\vec{x}) = P_{ij}$  when  $\zeta_t(\vec{x}) = H_i$ .

On the other hand, the parameters in the differential equation model are instantaneous rates of processes, and are unconstrained by space or time steps. In addition, competition in the differential equation model is more subtle. At any time point, all the competing

---

<sup>5</sup>Of course, the spatial model could be constructed in continuous time, in which case its parameters would be easier to interpret.

pathogens except for the one infecting  $v_{ij}$  can be removed and converted into empty space, and the instantaneous growth rate of  $v_{ij}$  would be totally unaffected. The effects of reduced competition are only evident at later times, when the hosts have been able to grow more freely in the absence of several pathogen strains, and as a result the remaining pathogen strain has more targets to infect. Similarly, in host-host competition for empty sites, the hosts in the differential equation model only inhibit one another's instantaneous growth by reducing the proportion of free space for colonization.

## 1.6 Limitations and Assumptions of This Formulation

Although this model is a good starting point for exploring the spatial effects in host-pathogen systems, it has many limitations and makes several assumptions which may not always be applicable. For example, in our model, some of the simplest and most far-reaching assumptions include: infected hosts can never give birth, uninfected hosts can never die, and multiple pathogens can never infect the same host. Removing any of these assumptions could uncover interesting new dynamics and reveal unexpected facts about corresponding real-world host-pathogen systems. It is important to keep these limitations in mind as we explore our system.

# Chapter 2

## Methods

### 2.1 Python Simulations

The spatial model was implemented in Python 2.6.6 using Eclipse version 4.2.1 and PyDev version 2.7.1. Simulations were run on a Hewlett-Packard TouchSmart TM2-2150US laptop with an Intel<sup>®</sup> Core<sup>™</sup> i3 U380 CPU. Wolfram Mathematica 9.0 was used for the graphical presentation of both analytic and imported simulation results and as an aid for algebraic manipulation as part of the analytic component of this project.

#### 2.1.1 Pathogen Spatial Evolution Simulations

For simulations of evolution in the spatial system, we start with a  $100 \times 100$  square lattice with roughly equal proportions of healthy and infected hosts at time  $t = 0$  (no empty sites). Within the populations of healthy and infected hosts, proportions of each particular species were roughly equal.

For pathogen-side evolution, we choose two parameters to vary in each simulation trial. For example, if we are examining pathogen-side evolution, we may vary  $\beta$  and  $\mu$  (pathogen-dependence only). The first iteration of our simulation would include a pathogen with a pre-specified set of parameters  $(\beta_1, \mu_1)$ , and a “mutated” pathogen with a new set of parameters within a defined radius of the original set,  $(\beta_2, \mu_2) = (\beta_1 + r_1, \mu_1 + r_2)$ , where  $\vec{r} = (r_1, r_2)$  and  $|\vec{r}|$  has been specified as a parameter of the simulation.

Then we simply run the simulation for a number of time steps and take a census of our system after the final step. Whichever pathogen has the highest numbers has “won” and will be retained for the next iteration of our simulation, in which it will compete with a new randomly generated competitor. In this way, we can track the system’s natural evolution over a fairly long time scale.

#### 2.1.2 Host Spatial Evolution Simulation Procedure

For pathogen-side evolution, it was easy to measure which pathogen was outcompeting the other. We simply counted the number of infected hosts for each pathogen type, and compared them. The pathogen with more infected hosts was more evolutionarily fit.

For host-side evolution, the situation is a little more complex. We have four species in simulation: two types of uninfected hosts and two corresponding types of infected hosts. We only have one type of pathogen. To assess the fitness of each host type, we need to take into account both the infected and uninfected populations. It is logical to just add them, since this represents the total population of that particular host type.

We now have a practical plan for comparing the fitness of two types of host (when one pathogen is present). We start with the same randomized scenario as we did for pathogen-side evolution, except with one more species in simulation. Then, we add together the infected and uninfected populations for each host type. Whichever host type is more numerous (regardless of the distribution of uninfected vs. infected individuals) at the end of our simulation is declared more fit.

### 2.1.3 Host Differential Equation Viability Simulations

For host-side evolution, it is difficult to find general analytic solutions, so we resort to numerical methods and assigning specific values to variables. To examine viability in the differential equation system, we first set several variables to constant values. We then used the `odeint`<sup>1</sup> function to solve our system numerically.

To test the viability of a new host species while in competition with a foundational species already in equilibrium with the pathogen, we started our new host off with no infected hosts and a very low population density of healthy host,  $10^{-10}$  in order to prevent perturbing the original equilibrium — for comparison, the population densities of the foundational host and infected host are on the order of  $10^{-1}$ .

We then used `odeint` to compute the infected and uninfected population densities for our new host at time  $t = 3$ . If the sum of the densities (the total density of new host) was greater than or equal to the original density of  $10^{-1}$ , we concluded that the new host was able to survive, and declared those parameter values to be viable.

### 2.1.4 Host Differential Equation Evolutionary Pressure

To compute a vector field for host evolution, we resorted to an exhaustive search. For evolution in a two-dimensional plane of two variables, we first set all other variables to constants. Then we overlaid a  $21 \times 21$  lattice over our plane, consisting of all points of the form  $(x_1, x_2) = (0.05n, 0.05m)$ , where  $n, m \in \mathbb{N}$  and  $0 \leq n, m \leq 20$ .

For each lattice point  $(x_1, x_2)$ , we computed the total population density of new hosts numerically after 3 units of time for 100 evenly spaced points on the circumference of a circle of radius 0.001 centered at  $(x_1, x_2)$ . Whichever set of parameters yields the largest total population in our numerical simulations is declared the direction of evolution. The vector from  $(x_1, x_2)$  to the winning point is extended for visibility. This procedure is repeated for all the lattice points, yielding a vector field by exhaustive search.

---

<sup>1</sup>This is a part of the Scipy, or Scientific Python, package, which can be found at [www.scipy.org/](http://www.scipy.org/).

# Chapter 3

## Results

In each section, we will begin with analytic work on the differential equation model, and use the results to inform our choices of initial conditions and parameters for the simulation.

### 3.1 Evolution on the Pathogen Side

To analytically investigate competition between two strains of pathogens and assess relative fitness, we decided to use the criteria of invadability. Suppose we have one strain of host and one strain of pathogen, call it pathogen A, in equilibrium. Then, if pathogen B increases (or at least does not decrease) in number when we introduce it in a very small quantity, we say that B invades A. If B invades A and A invades B, then it follows that A and B can coexist, and therefore A and B are equally fit in some sense. On the other hand, if B invades A but A cannot invade B, then B is more fit than A and evolution will tend to move in the direction of the parameters of strain B over those of strain A.

We begin by establishing an equilibrium in the differential equation system between one host species and one pathogen species. In this case, we have:

$$\frac{du}{dt} = \alpha u(1 - u - v) - \beta uv + \gamma v = 0; \quad (3.1.1)$$

$$\frac{dv}{dt} = \beta uv - (\gamma + \mu)v = 0. \quad (3.1.2)$$

Looking at the second equation, we notice that if  $v$  is positive, we can divide by it to see that in equilibrium, we must have

$$\beta u - (\gamma + \mu) = 0; \quad (3.1.3)$$

$$\bar{u} = \frac{\gamma + \mu}{\beta}. \quad (3.1.4)$$

Now, enforcing (3.1.1), we get that

$$\alpha \bar{u} - \alpha \bar{u}^2 - \alpha \bar{u}v - \beta \bar{u}v + \gamma v = 0; \quad (3.1.5)$$

$$\alpha \bar{u} - \alpha \bar{u}^2 = (\alpha \bar{u} + \beta \bar{u} - \gamma) v; \quad (3.1.6)$$

$$v = \frac{\alpha \bar{u} - \alpha \bar{u}^2}{\alpha \bar{u} + \beta \frac{\gamma + \mu}{\beta} - \gamma}; \quad (3.1.7)$$

$$\bar{v} = \frac{\alpha \bar{u} (1 - \bar{u})}{\alpha \bar{u} + \mu}. \quad (3.1.8)$$

We also realize that since the maximum possible value of  $\bar{u}$  is 1, (3.1.4) is only possible for nonzero  $v$  when

$$\beta > \gamma + \mu. \quad (3.1.9)$$

We now see that equation (3.1.9) defines the general viable region for pathogens.

## 3.2 Pathogen $\mu$ - $\beta$ Evolution

In general, pathogens will tend to evolve toward lower virulence ( $\mu$ ) and higher transmissibility ( $\beta$ ), since virulence is a mechanism for decreasing the density of infected hosts, while transmission is a mechanism for increasing the infected population.

### 3.2.1 Viable Region

First, we plot the viable region, given in (3.1.9) in the  $\mu$ - $\beta$  plane of parameter space, where pathogens persist in the long term and do not die off, shown in Figure 3.1.

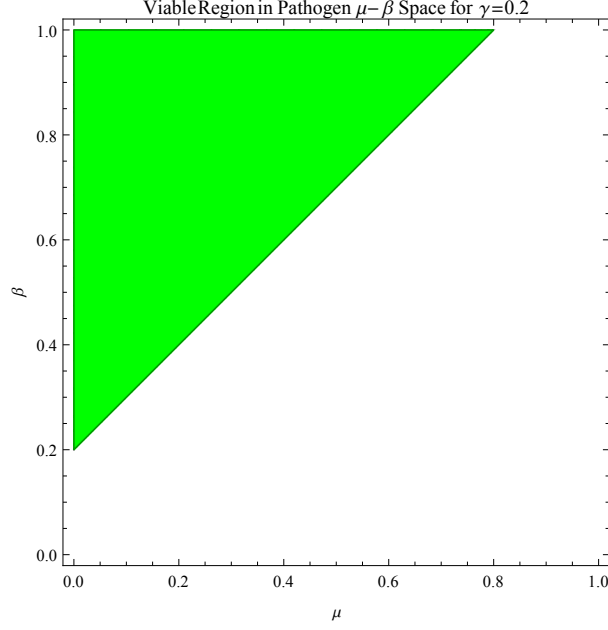


Figure 3.1: The shaded green area is the region of  $\mu$ - $\beta$  parameter space in which pathogens are viable. We see that the  $\beta$ -intercept of the border is found at  $\beta = \gamma$ , and that the border has a slope of 1.

### 3.2.2 Fitness

As mentioned earlier, we will discuss fitness using the criteria of invadability. If we introduce a second pathogen species to our system of one host and one pathogen in equilibrium, and our second species is able to increase when its population density is low, then it is able to invade the first. Let's find the criteria that make this possible. We begin with a system in equilibrium:

$$\frac{du}{dt} = \alpha u(1 - u - v_1) - \beta_1 uv_1 + \gamma v_1 = 0; \quad (3.2.1)$$

$$\frac{dv_1}{dt} = \beta_1 uv_1 - (\gamma + \mu_1) v_1 = 0. \quad (3.2.2)$$

Here in equations 3.2.1 and 3.2.2, we have discarded all subscripts relating to host-dependence of parameters (there is only one type of host) and all subscripts for the parameters not being evolved, such as  $\gamma$  (these parameters are the same for all species in our system). In equilibrium, we have, as before:

$$\bar{u} = \frac{\gamma + \mu_1}{\beta_1}; \quad (3.2.3)$$

$$\bar{v}_1 = \frac{\alpha \bar{u}(1 - \bar{u})}{\alpha \bar{u} + \mu_1}. \quad (3.2.4)$$



Introducing a small density of a second pathogen into the system without disturbing the original equilibrium, we have that the growth of the second type of infected host is given by

$$\frac{dv_2}{dt} = \beta_2 \bar{u} v_2 - (\gamma + \mu_2) v_2. \quad (3.2.5)$$

Now let's find the conditions that are sufficient to allow our second pathogen to invade this system and persist. Therefore, we require that

$$\frac{dv_2}{dt} = \beta_2 \bar{u} v_2 - (\gamma + \mu_2) v_2 > 0. \quad (3.2.6)$$

It follows that

$$\beta_2 \frac{\gamma + \mu_1}{\beta_1} v_2 - (\gamma + \mu_2) v_2 > 0; \quad (3.2.7)$$

$$\frac{\beta_2}{\mu_2 + \gamma} > \frac{\beta_1}{\mu_1 + \gamma}. \quad (3.2.8)$$

Now, for simplicity, we consider the case in which  $\gamma = 0$ . In this case, we have that

$$\frac{\beta_2}{\mu_2} > \frac{\beta_1}{\mu_1}. \quad (3.2.9)$$

So, we now see that when inequality (3.2.9) holds, pathogen 2 can invade an equilibrium system of pathogen 1 and host. Further, when we have the degenerate case of

$$\frac{\beta_2}{\mu_2} = \frac{\beta_1}{\mu_1}, \quad (3.2.10)$$

instead, we have that

$$\frac{dv_2}{dt} = \frac{dv_1}{dt} = 0. \quad (3.2.11)$$

In this case, it is clear that neither pathogen strain will outcompete the other. Instead, they are able to coexist indefinitely. As a result, we realize that all pathogens with parameters along a line

$$\frac{\beta}{\mu} = c, \text{ with } c = \text{constant} \quad (3.2.12)$$

have equal fitness, and that pathogens along lines with higher values of  $c$  are more fit and can invade those along lines with lower values of  $c$ . So, it is reasonable to use the value of  $c$  as a measure of fitness, and we have graphed several lines of equal fitness in Figure 3.2.

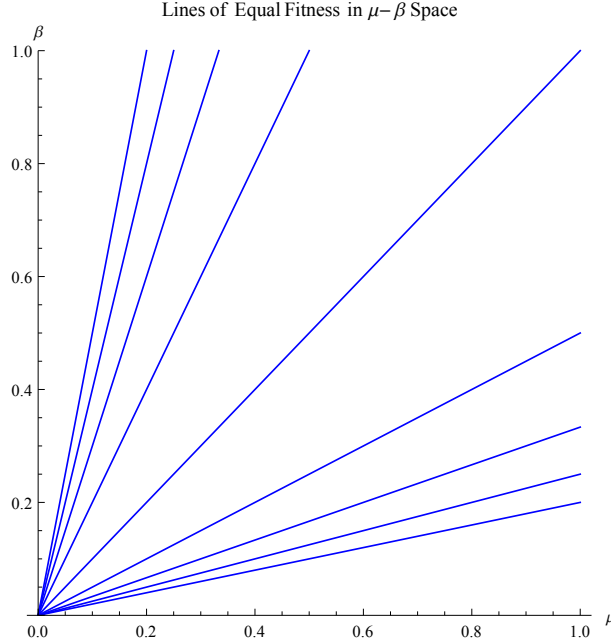


Figure 3.2: Here we have several lines of equal fitness in the  $\mu$ - $\beta$  plane for pathogens. Their equations are all of the form  $\frac{\beta}{\mu} = c$ , where  $c$  is a constant.

### 3.2.3 Direction of Evolution

Now that we have defined lines of equal fitness, we realize that the direction of evolutionary pressure must be perpendicular to these lines. So, at any general point  $(\mu_0, \beta_0)$  in parameter space, we know that the line of constant fitness through that point is given by

$$\beta = \frac{\beta_0}{\mu_0} \mu \quad (3.2.13)$$

and has slope  $\frac{\beta_0}{\mu_0}$ . Since a line perpendicular to a line of slope  $b$  has slope  $-1/b$ , and the direction of evolution is perpendicular to the line of constant fitness, we have that at  $(\mu_0, \beta_0)$ , the direction of evolution has slope  $-\frac{\mu_0}{\beta_0}$ .

Using Mathematica to normalize the magnitudes of these vectors (we're not sure how strong evolutionary pressure is at each point; we only know the direction) and produce a plot of this vector field, we see that evolution in the  $\mu$ - $\beta$  plane generally follows the vector field in Figure 3.3.

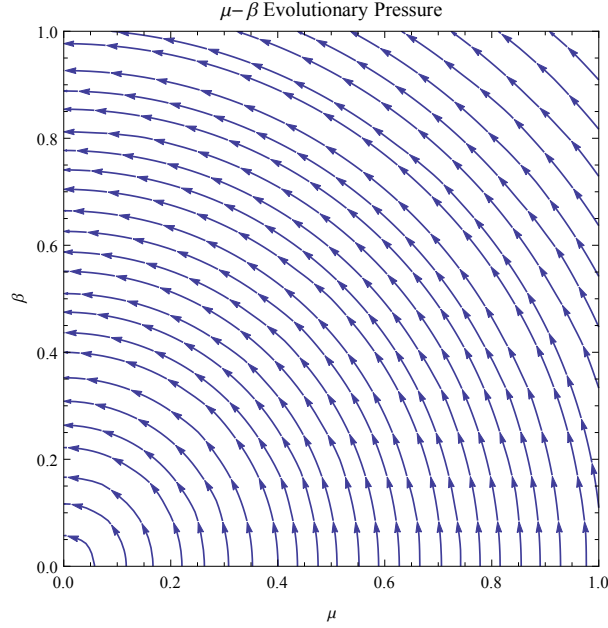


Figure 3.3: This plot displays the direction of evolutionary pressure in the  $\mu$ - $\beta$  plane. In general, pathogens evolve towards lower virulence and higher transmissibility, resulting in the pattern of concentric partial circles seen here. Note that there is evolutionary pressure even in the non-viable region of the plane. Although those dynamics are often difficult to observe due to the evolutionary time-scale being longer than the time-scale for the pathogen to die out, the pressure is still present.

### 3.2.4 Spatial Evolution Simulation

Now that we know what evolution looks like in the mean field equation, we can use it as a first guess for what evolution will look like in the spatial model. Based on the vector field lines in Figure 3.3, we can choose starting points for our spatial simulations that give us a representative look at the direction of evolutionary pressure in the V-T (spatial model names for  $\mu$ - $\beta$ ) plane. We see this in Figure 3.4.

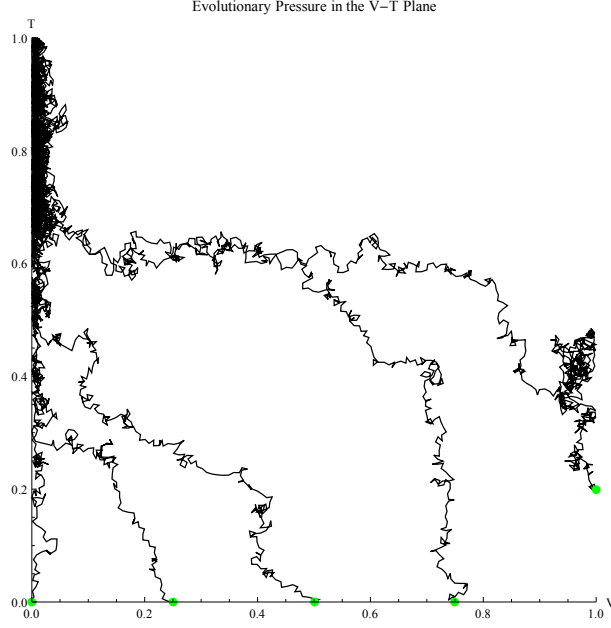


Figure 3.4: This plot shows the result of simulations starting at  $(V, T) = (0.0, 0.0)$ ,  $(0.25, 0.0)$ ,  $(0.50, 0.0)$ ,  $(0.75, 0.0)$ , and  $(1.0, 0.2)$ , with 2000 time steps for each starting point. The small green dots indicate starting parameters, and the black lines mark the evolutionary trajectory.

### 3.3 Pathogen $\gamma$ - $\beta$ Evolution

If we look at the general equation for infected host population density (3.1.2), we realize that  $\gamma$  and  $\mu$  are equivalent in terms of their effect on pathogen fitness, invadability, and viability. So, the results of this section are entirely analogous to those of the previous one.

#### 3.3.1 Viable Region

The viable region in  $\gamma$ - $\beta$  space for a particular value of  $\mu$  is shown in Figure 3.5.

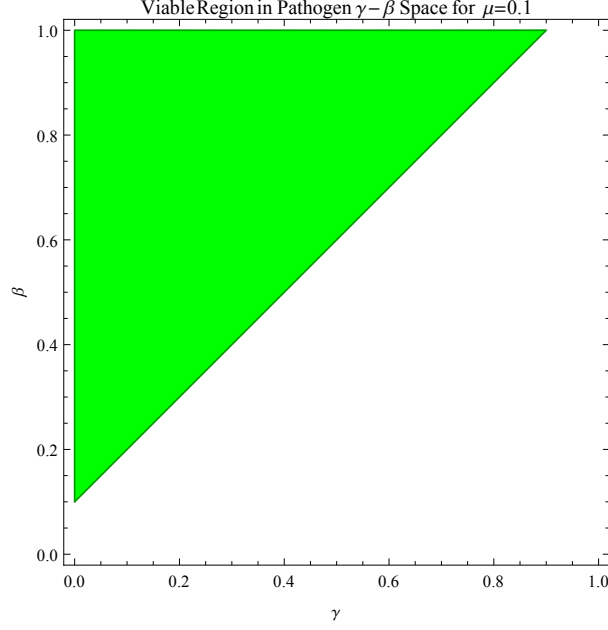


Figure 3.5: The shaded green area is the region of  $\gamma$ - $\beta$  parameter space in which pathogens are viable. We see that the  $\beta$ -intercept of the border is found at  $\beta = \mu$ , and that the border has a slope of 1.

### 3.3.2 Fitness

The lines of equal fitness in the  $\gamma$ - $\beta$  plane are essentially analogous to those in the  $\mu$ - $\beta$  plane. However, let's confirm this directly. When  $\mu$  and  $\beta$  are allowed to evolve, we see that the equations governing a single host and pathogen strain in equilibrium are given by

$$\frac{du}{dt} = \alpha u (1 - u - v_1) - \beta_1 u v_1 + \gamma_1 v_1 = 0; \quad (3.3.1)$$

$$\frac{dv_1}{dt} = \beta_1 u v_1 - (\gamma_1 + \mu) v_1 = 0; \quad (3.3.2)$$

$$\bar{u} = \frac{\gamma_1 + \mu}{\beta_1}; \quad (3.3.3)$$

$$\bar{v}_1 = \frac{\alpha \bar{u} (1 - \bar{u})}{\alpha \bar{u} + \mu}, \quad (3.3.4)$$

where we have removed all unnecessary subscripts. Introducing a second pathogen and following the same procedure as we did for fitness in the  $\mu$ - $\beta$  plane, we find that in order to have a second pathogen invade successfully,

$$\frac{dv_2}{dt} = \beta_2 \bar{u} v_2 - (\gamma_2 + \mu) v_2 > 0, \quad (3.3.5)$$

we must have

$$\frac{\beta_2}{\gamma_2 + \mu} > \frac{\beta_1}{\gamma_1 + \mu}. \quad (3.3.6)$$

To once again simplify the situation, we set  $\mu = 0$ , and see that

$$\frac{\beta_2}{\gamma_2} > \frac{\beta_1}{\gamma_1}. \quad (3.3.7)$$

So, we see that the lines of equal fitness in the  $\gamma$ - $\beta$  plane are of the same form as those in (3.2.12), but with the  $\mu$  replaced by a  $\gamma$ .

$$\frac{\beta}{\gamma} = c, \text{ with } c = \text{constant} \quad (3.3.8)$$

Graphing (3.3.8) for a few different values of  $c$ , we get Figure 3.6.

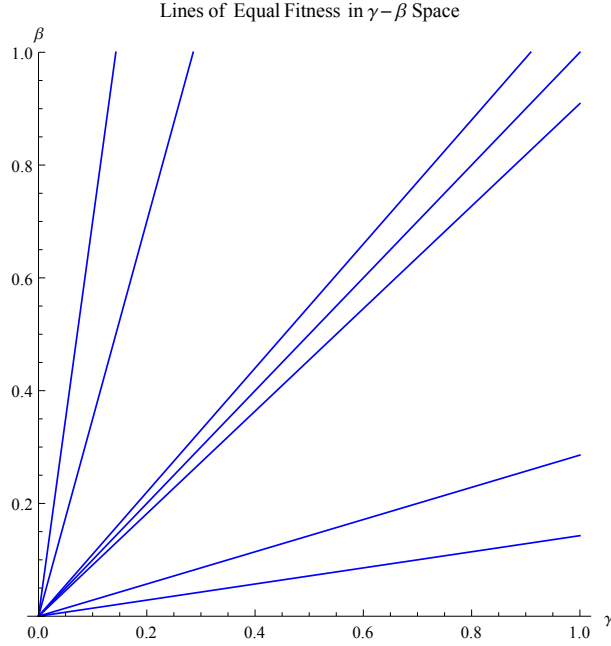


Figure 3.6: Here we have several lines of equal fitness in the  $\gamma$ - $\beta$  plane for pathogens. Their equations are all of the form  $\frac{\beta}{\gamma} = c$ , where  $c$  is a constant.

### 3.3.3 Direction of Evolution

Going through the same process we did for the  $\mu$ - $\beta$  plane, we see in Figure 3.7 that evolution for pathogens is essentially identical in the  $\gamma$ - $\beta$  plane.

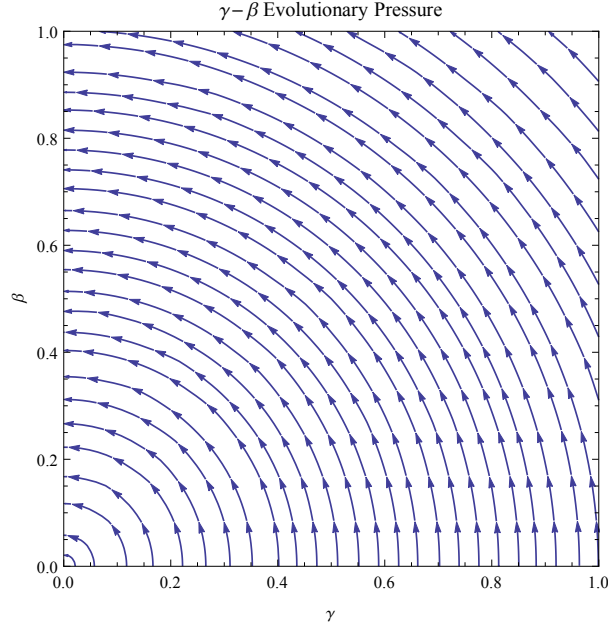


Figure 3.7: This plot displays the direction of evolutionary pressure in the  $\gamma$ - $\beta$  plane, essentially the same as the direction in the  $\mu$ - $\beta$  plane.

### 3.3.4 Spatial Evolution Simulation

Although the instantaneous evolutionary vector field we found using the differential equation system looks identical to the field for the  $\mu$ - $\beta$  plane, it is important to note that the spatial model may reveal important differences. It is clear that V and R are different parameters; while both of them decrease the density and population of infected hosts, V replaces them with empty sites, while R replaces them with healthy hosts, which can be immediately recolonized. Figure 3.8 shows some of the evolutionary dynamics.

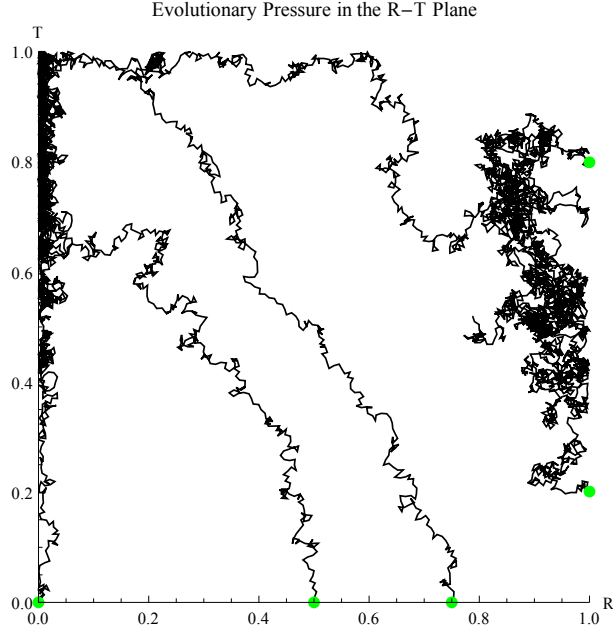


Figure 3.8: This plot shows the result of simulations starting at  $(R, T) = (0.0, 0.0), (1.0, 0.8), (0.50, 0.0), (0.75, 0.0), (1.0, 0.2)$ , with 2000 time steps for each starting point.

### 3.4 Pathogen $\mu$ - $\gamma$ Evolution

We have just seen that evolutionary pressure is symmetric with respect to the  $\mu$ - $\beta$  and  $\gamma$ - $\beta$  planes for pathogens. This is a result of the symmetry between  $\gamma$  and  $\mu$  in the differential equation governing the population density of infected hosts. As a result of this symmetry, we expect that evolution in the  $\mu$ - $\gamma$  plane will be actually symmetric over the line  $\gamma = \mu$ .

#### 3.4.1 Viable Region

Applying equation (3.1.9) for a specific value of  $\beta$ , we produce Figure 3.9.



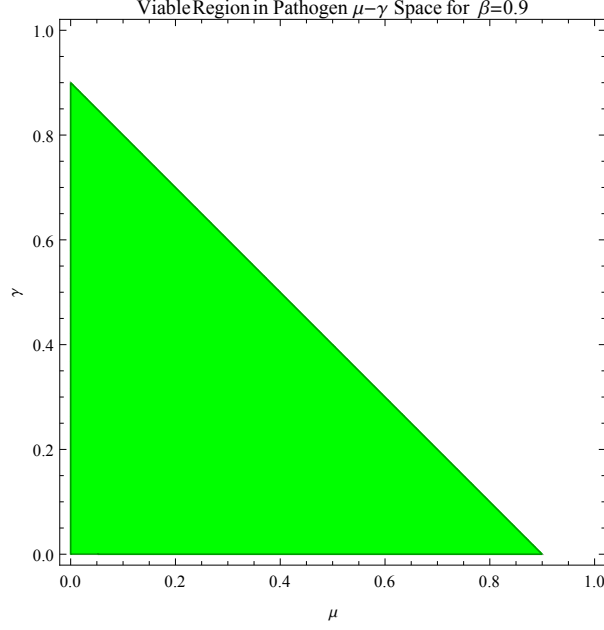


Figure 3.9: The viable region in  $\mu$ - $\gamma$  space for  $\beta = 0.9$ . As expected, it is symmetric over the line  $\gamma = \mu$ . The border has a slope of  $-1$  and intersects both axes at the value of  $\beta$ .

### 3.4.2 Fitness

To define a metric of fitness in the  $\mu$ - $\gamma$  plane, we begin with a single host and single pathogen in equilibrium, as usual.

$$\frac{du}{dt} = \alpha u (1 - u - v_1) - \beta u v_1 + \gamma_1 v_1 = 0 \quad (3.4.1)$$

$$\frac{dv_1}{dt} = \beta_1 u v_1 - (\gamma_1 + \mu) v_1 = 0 \quad (3.4.2)$$

$$\bar{u} = \frac{\gamma_1 + \mu_1}{\beta} \quad (3.4.3)$$

$$\bar{v}_1 = \frac{\alpha \bar{u} (1 - \bar{u})}{\alpha \bar{u} + \mu_1} \quad (3.4.4)$$

Now, let's assume that a second pathogen is able to invade the first, and try to obtain a sufficient condition for this.

$$\frac{dv_2}{dt} = \beta \bar{u} v_2 - (\gamma_2 + \mu_2) v_2 > 0 \quad (3.4.5)$$

$$\gamma_2 + \mu_2 < \gamma_1 + \mu_1 \quad (3.4.6)$$

We quickly see that (3.4.6) gives the condition for declaring one pathogen more fit than another in this plane. Therefore, it follows that lines of equal fitness are given by

$$\mu + \gamma = c, \text{ with } c = \text{constant.} \quad (3.4.7)$$

Several such lines are drawn in Figure 3.10.

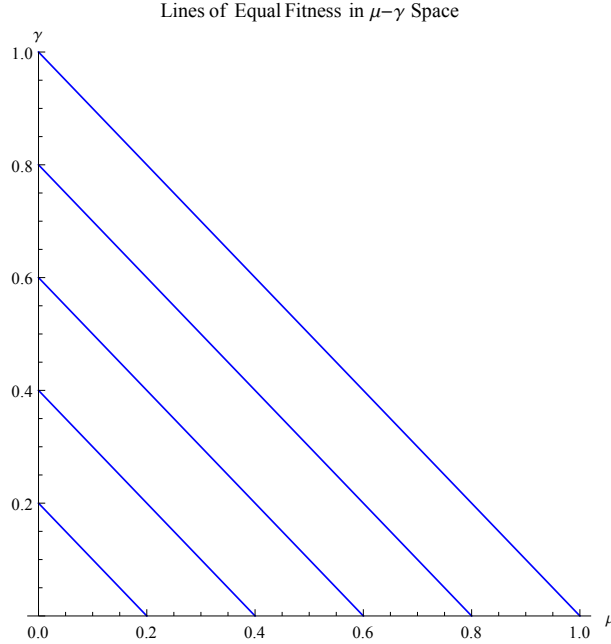


Figure 3.10: Lines of equal fitness in the  $\mu$ - $\gamma$  plane for pathogens.

### 3.4.3 Direction of Evolution

From the previous subsection, we see that lines of constant fitness through a point  $(\mu_0, \gamma_0)$  have slope  $-\mu_0$ . Since evolutionary pressure is perpendicular to lines of constant fitness, we realize that at each point  $(\mu_0, \gamma_0)$ , the vector of evolutionary pressure must have slope  $1/\mu_0$ . Using the fact that pathogens will generally evolve toward lower virulence and recovery, we plot a normalized vector field in Mathematica, shown in Figure 3.11.

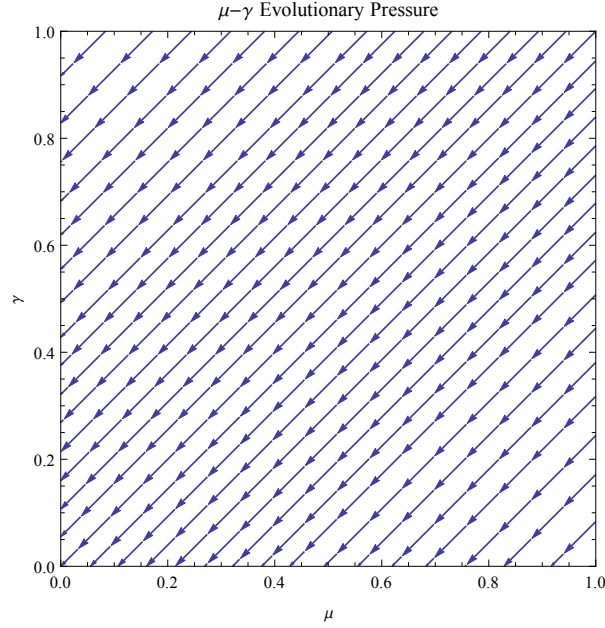


Figure 3.11: This plot displays the direction of evolutionary pressure in the  $\mu$ - $\gamma$  plane for pathogens.

### 3.4.4 Spatial Evolution Simulation

Evolution in this plane is different from the two previous cases. Again using the vector field from our differential equation model as a guide, we choose points to try to obtain representative evolutionary trajectories. Interestingly, we see that the non-viable region in  $\mu$ - $\gamma$  space seems to be more non-viable than the region in other spaces. In that region, our evolutionary trajectories tend to resemble random walks! Some of these simulation results are shown in Figure 3.12.

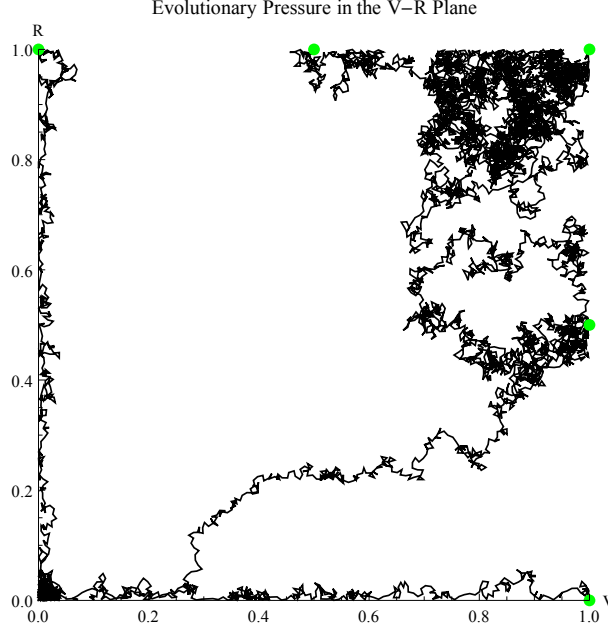


Figure 3.12: This plot shows the result of simulations starting at  $(V, R) = (1.0, 0.0), (1.0, 1.0), (0.0, 1.0), (1.0, 0.5), (0.5, 1.0)$ , with 2000 time steps for each starting point.

## 3.5 Evolution on the Host Side

Now, evolution on the host side is slightly different from evolution on the pathogen side. When we were examining invadability, coexistence, and fitness of different pathogen strains, we only had to deal with a system with three distinct species: a single host type, and the two pathogen types we were comparing. When comparing the fitness of two species of hosts, our system has a minimum of two types of hosts and two types of infected hosts.

### 3.5.1 Preliminary Analysis for $\alpha$ - $\beta$ Evolution

So, to investigate the evolution of the growth and transmissibility parameters as properties of host types, we begin with a two-species (one pathogen, one host) differential equation system.

$$\frac{du_1}{dt} = \alpha_1 u_1 (1 - u_1 - v_1) - \beta_1 u_1 v_1 + \gamma v_1 \quad (3.5.1)$$

$$\frac{dv_1}{dt} = \beta_1 u_1 v_1 - (\gamma + \mu) v_1 \quad (3.5.2)$$

In equilibrium, we have, as before:

$$\overline{u_1} = \frac{\gamma + \mu}{\beta_1}; \quad (3.5.3)$$

$$\bar{v}_1 = \frac{(\alpha_1 \bar{u}_1)(1 - \bar{u}_1)}{\alpha_1 \bar{u}_1 + \mu} = \frac{(1 - \bar{u}_1)}{1 + \frac{\mu}{\alpha_1 \bar{u}_1}} = \frac{\frac{\beta_1 - \gamma - \mu}{\beta_1}}{\frac{\gamma + \mu + \beta_1 \mu}{\gamma + \mu}} = \frac{(\gamma + \mu)(\beta_1 - \gamma - \mu)}{\beta_1(\gamma + \mu + \beta_1 \mu)}. \quad (3.5.4)$$

Now, if we introduce a new host — and along with it, a new infected host/pathogen — in a small enough quantity to not disturb the original equilibrium, we have:

$$\frac{du_2}{dt} = \alpha_2 u_2 (1 - \bar{u}_1 - u_2 - \bar{v}_1 - v_2) - \beta_2 (\bar{v}_1 + v_2) u_2 + \gamma v_2; \quad (3.5.5)$$

$$\frac{dv_2}{dt} = \beta_2 u_2 (\bar{v}_1 + v_2) - (\gamma + \mu) v_2. \quad (3.5.6)$$

Rearranging and consolidating the terms in the previous equations, we get:

$$\frac{du_2}{dt} = (\alpha_2 - \alpha_2 \bar{u}_1 - \alpha_2 \bar{v}_1 - \beta_2 \bar{v}_1) u_2 + \gamma v_2 - \alpha_2 u_2 (u_2 + v_2) - \beta_2 v_2 u_2; \quad (3.5.7)$$

$$\frac{dv_2}{dt} = \beta_2 \bar{v}_1 u_2 - (\gamma + \mu) v_2 + v_2 u_2. \quad (3.5.8)$$

Recall that we chose  $u_2$  and  $v_2$  to be small in order to not disrupt the original equilibrium. We notice, however, that if  $u_2$  and  $v_2$  are of order  $\epsilon$ , terms with higher powers of  $u_2$  and/or  $v_2$  are of order  $\epsilon^2$  or smaller, and in most cases are of negligible magnitude compared to other terms.

$$\frac{du_2}{dt} = (\alpha_2 - \alpha_2 \bar{u}_1 - \alpha_2 \bar{v}_1 - \beta_2 \bar{v}_1) u_2 + \gamma v_2 \quad (3.5.9)$$

$$\frac{dv_2}{dt} = \beta_2 \bar{v}_1 u_2 - (\gamma + \mu) v_2 \quad (3.5.10)$$

We now have a linear system of ordinary differential equations, and can solve it by examining the system in vector form and finding the eigenvalues of the matrix of coefficients.

$$\begin{bmatrix} \frac{du_2}{dt} \\ \frac{dv_2}{dt} \end{bmatrix} = \begin{bmatrix} \alpha_2 - \alpha_2 \bar{u}_1 - \alpha_2 \bar{v}_1 - \beta_2 \bar{v}_1 & \gamma \\ \beta_2 \bar{v}_1 & -\gamma - \mu \end{bmatrix} \begin{bmatrix} u_2 \\ v_2 \end{bmatrix} \quad (3.5.11)$$

Let's call this matrix  $A$ , and let's replace the  $\bar{u}_1$ 's and  $\bar{v}_1$ 's in it with their values in terms of our parameters  $\alpha, \beta, \gamma, \mu$ .

$$A = \begin{bmatrix} \alpha_2 - \alpha_2 \left( \frac{\gamma + \mu}{\beta_1} \right) - \alpha_2 \frac{(\gamma + \mu)(\beta_1 - \gamma - \mu)}{\beta_1(\gamma + \mu + \beta_1 \mu)} - \beta_2 \frac{(\gamma + \mu)(\beta_1 - \gamma - \mu)}{\beta_1(\gamma + \mu + \beta_1 \mu)} & \gamma \\ \beta_2 \frac{(\gamma + \mu)(\beta_1 - \gamma - \mu)}{\beta_1(\gamma + \mu + \beta_1 \mu)} & -\gamma - \mu \end{bmatrix} \quad (3.5.12)$$

Using Mathematica to view the eigenvalues of  $A$  when we manipulate the six parameters, we see that it is possible to have two positive eigenvalues (see equation 3.5.13), two negative eigenvalues (see equation 3.5.14), one positive and one negative (see equation 3.5.15), or even complex eigenvalues (see equation 3.5.16), implying that this system can exhibit a diverse range of behavior.

$$(\alpha_1, \beta_1, \mu, \gamma, \alpha_2, \beta_2) = (0.059, 0.022, 0.196, 0.339, 0.725, 0.196) \quad (3.5.13)$$

$$(\alpha_1, \beta_1, \mu, \gamma, \alpha_2, \beta_2) = (0.455, 0.201, 0.075, 0.048, 0.038, 0.059) \quad (3.5.14)$$

$$(\alpha_1, \beta_1, \mu, \gamma, \alpha_2, \beta_2) = (0.059, 0.027, 0.075, 0.048, 0.038, 0.059) \quad (3.5.15)$$

$$(\alpha_1, \beta_1, \mu, \gamma, \alpha_2, \beta_2) = (0.159, 0.233, 0.524, 0.503, 0.408, 0.397) \quad (3.5.16)$$

### 3.5.2 Approach to Host Side Evolution

Since even the differential equation system is somewhat intractable analytically, we will make some simplifications and try to understand what happens in a more specific setting. Since we cannot fully answer the general question of how evolution in a parameter space with two host-side variables depends on the other four parameters, we will fix most parameters and observe the behavior of the system.

For each possible pair of host-side parameters, we begin with a spatial simulation where the pair is allowed to evolve, while all other parameters are held fixed at previously chosen values. In order to examine a diverse sample of parameter space, the constant parameters for each pair of evolving parameters were individually set.

Next, we examine viability in the differential equation system by starting with a system with a fixed constant amount of the foundational  $u_1$  and  $v_1$  species, then perturbing it with a very small amount of a competing host,  $u_2$ . Then we numerically solve the system of equations up to time  $t = 3$ , and see how the total amount of competing host (both uninfected and infected),  $u_2 + v_2$ , has changed from our original perturbation. For the viability simulations, we used a consistent set of constant parameters across all evolving parameter pairs. Whenever parameters were fixed as constants, the scheme in equation 3.5.17 was used.

$$\begin{aligned} u_{1\text{avg}} &= v_{1\text{avg}} = 0.4 \\ \alpha_2 &= 0.6 \\ \beta_2 &= 0.7 \\ \gamma_2 &= 0.3 \\ \mu_2 &= 0.2 \end{aligned} \quad (3.5.17)$$

Lastly, we use an exhaustive search method to obtain an estimate of the direction of evolutionary pressure in the differential system. For 441 points in the plane, we test host population growth in 100 different directions in a neighborhood of the point, then choose the direction of greatest increase to plot in our vector field.

### 3.6 Host $\alpha$ - $\beta$ Evolution

For host-side  $\alpha$ - $\beta$  evolution, we expect evolutionary pressure to generally tend towards higher  $\alpha$  and lower  $\beta$ . Higher  $\alpha$  is beneficial because it directly increases the host population. Higher  $\beta$  is detrimental because it converts a healthy host, with the potential for growth, to an infected host, which cannot grow and can only die or recover. Therefore we expect lower  $\beta$  to be beneficial. The simulation results for the host  $\alpha$ - $\beta$  plane are shown in Figure 3.13.

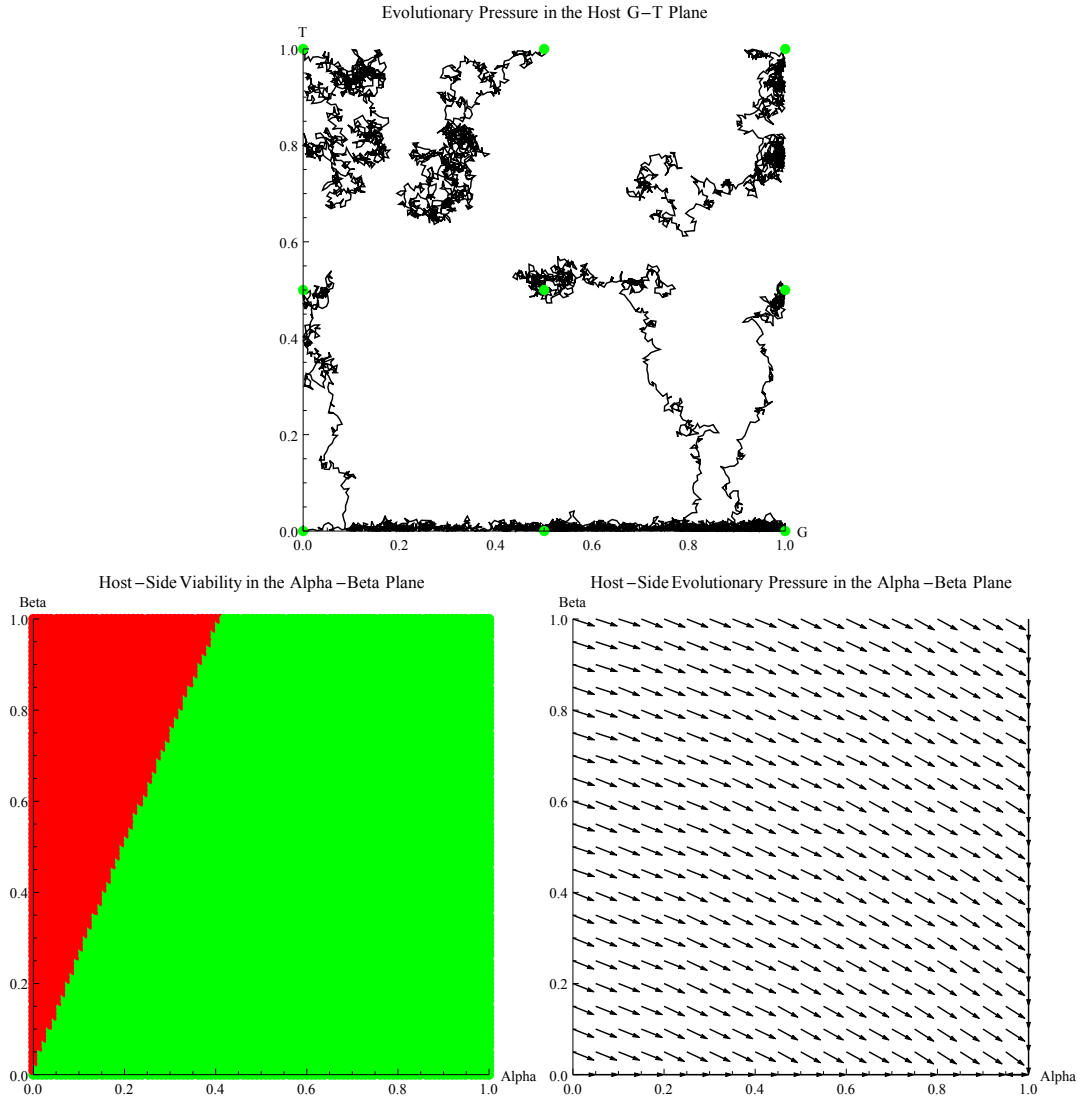


Figure 3.13: Left: This plot shows the result of simulations starting at  $(G, T) = (0.0, 0.0)$ ,  $(0.0, 0.5)$ ,  $(0.0, 1.0)$ ,  $(0.5, 0.0)$ ,  $(0.5, 0.5)$ ,  $(0.5, 1.0)$ ,  $(1.0, 0.0)$ ,  $(1.0, 0.5)$ ,  $(1.0, 1.0)$ , with 2000 time steps for each starting point. In this spatial simulation, the fixed parameters were  $V = 0.3$  and  $R = 0.1$ . Center: This plot shows the viable region (green) and nonviable region (red) of the host-side  $\alpha$ - $\beta$  plane. Right: The evolutionary pressure vector field computed from the ODE system.

### 3.7 Host $\alpha$ - $\gamma$ Evolution

For host-side  $\alpha$ - $\gamma$  evolution, we expect evolutionary pressure to generally tend towards higher  $\alpha$  and higher  $\gamma$ . Higher  $\alpha$  is beneficial for reasons stated earlier. Higher  $\gamma$  is beneficial because it converts an infected host, which cannot grow and can only die or recover, to a healthy host, which cannot die and has the potential for growth. The simulation results for the host  $\alpha$ - $\gamma$  plane are shown in Figure 3.14.

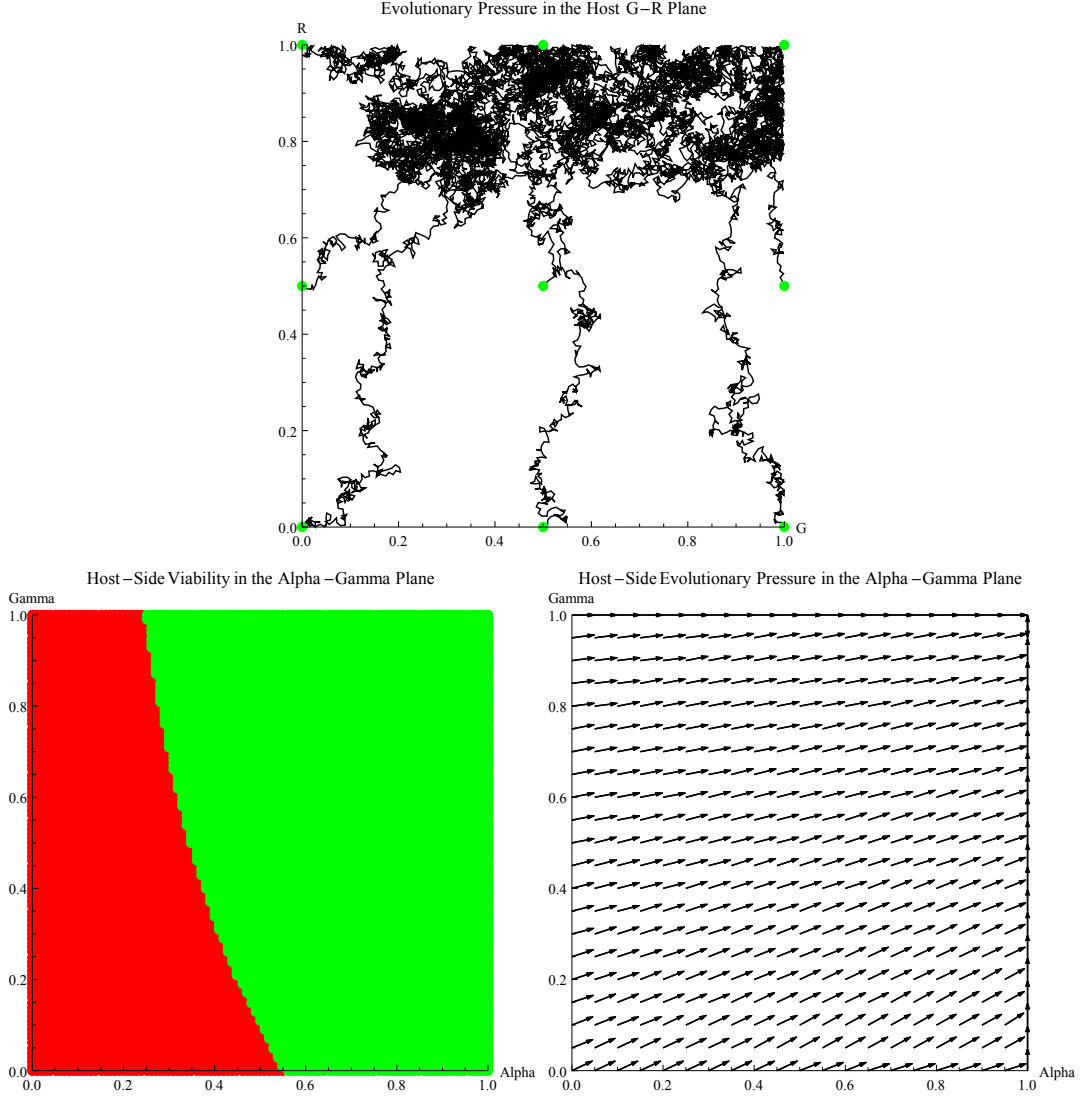


Figure 3.14: Left: This plot shows the result of simulations starting at  $(G, R) = (0.0, 0.0)$ ,  $(0.0, 0.5)$ ,  $(0.0, 1.0)$ ,  $(0.5, 0.0)$ ,  $(0.5, 0.5)$ ,  $(0.5, 1.0)$ ,  $(1.0, 0.0)$ ,  $(1.0, 0.5)$ ,  $(1.0, 1.0)$ , with 2000 time steps for each starting point. In this spatial simulation, the fixed parameters were  $V = 0.3$  and  $R = 0.6$ . Center: This plot shows the viable region (green) and nonviable region (red) of the host-side  $\alpha$ - $\gamma$  plane. Right: The evolutionary pressure vector field computed from the ODE system.



### 3.8 Host $\alpha$ - $\mu$ Evolution

For host-side  $\alpha$ - $\mu$  evolution, we expect evolutionary pressure to generally tend towards higher  $\alpha$ . Higher  $\alpha$  is beneficial for reasons mentioned earlier. The role of  $\mu$ , however is more difficult to predict. Higher  $\mu$  is detrimental in that it decreases the overall host population by killing off infected hosts. However, it may be beneficial by leaving behind an empty site, which is now available for colonization by healthy hosts. Therefore, it is likely that the direction of evolutionary pressure in the parameter  $\mu$  will vary based on the values of the other parameters. The simulation results for the host  $\alpha$ - $\mu$  plane are shown in Figure 3.15.

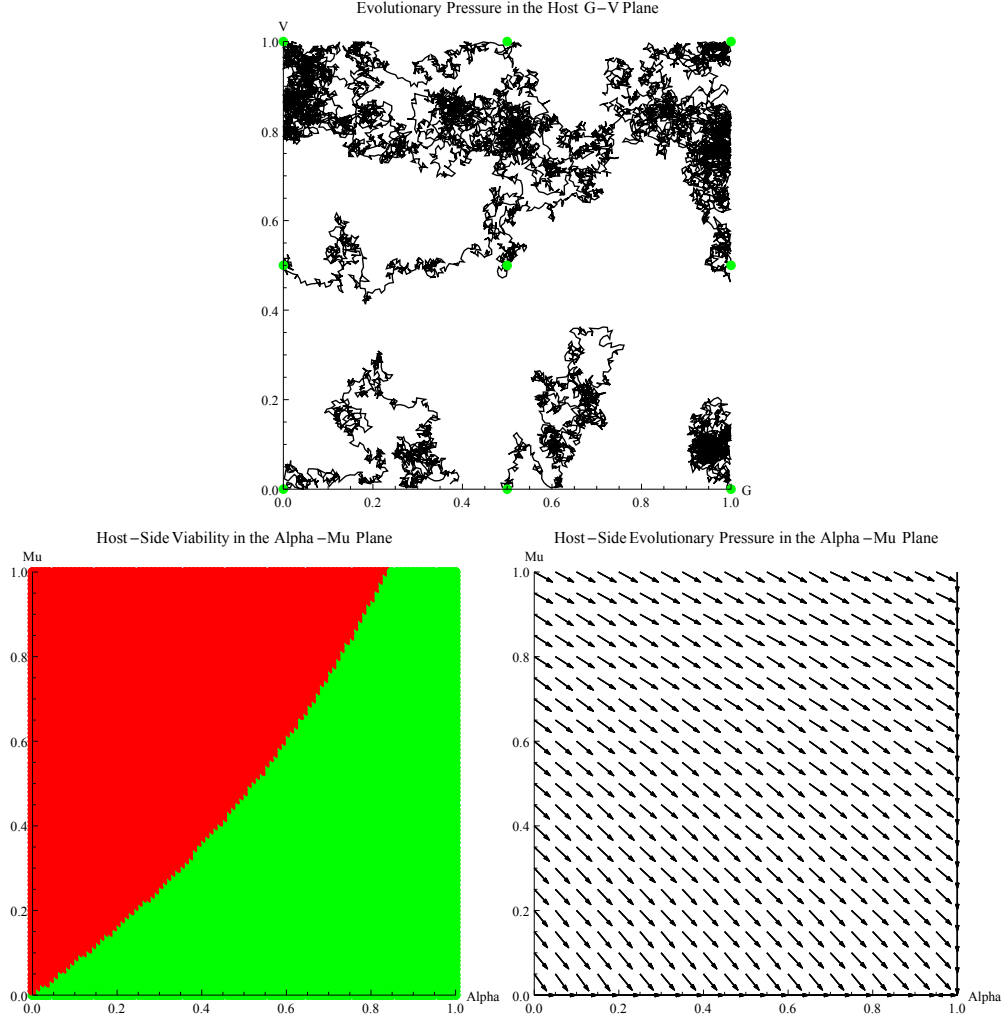


Figure 3.15: Left: This plot shows the result of simulations starting at  $(G, V) = (0.0, 0.0)$ ,  $(0.0, 0.5)$ ,  $(0.0, 1.0)$ ,  $(0.5, 0.0)$ ,  $(0.5, 0.5)$ ,  $(0.5, 1.0)$ ,  $(1.0, 0.0)$ ,  $(1.0, 0.5)$ ,  $(1.0, 1.0)$ , with 2000 time steps for each starting point. In this spatial simulation, the fixed parameters were  $T = 0.6$  and  $R = 0.25$ . Center: This plot shows the viable region (green) and nonviable region (red) of the host-side  $\alpha$ - $\mu$  plane. Right: The evolutionary pressure vector field computed from the ODE system.

### 3.9 Host $\beta$ - $\gamma$ Evolution

For host-side  $\beta$ - $\gamma$  evolution, we expect evolutionary pressure to generally tend towards lower  $\beta$  and higher  $\gamma$ , for reasons mentioned earlier. The simulation results for the host  $\beta$ - $\gamma$  plane are shown in Figure 3.16.

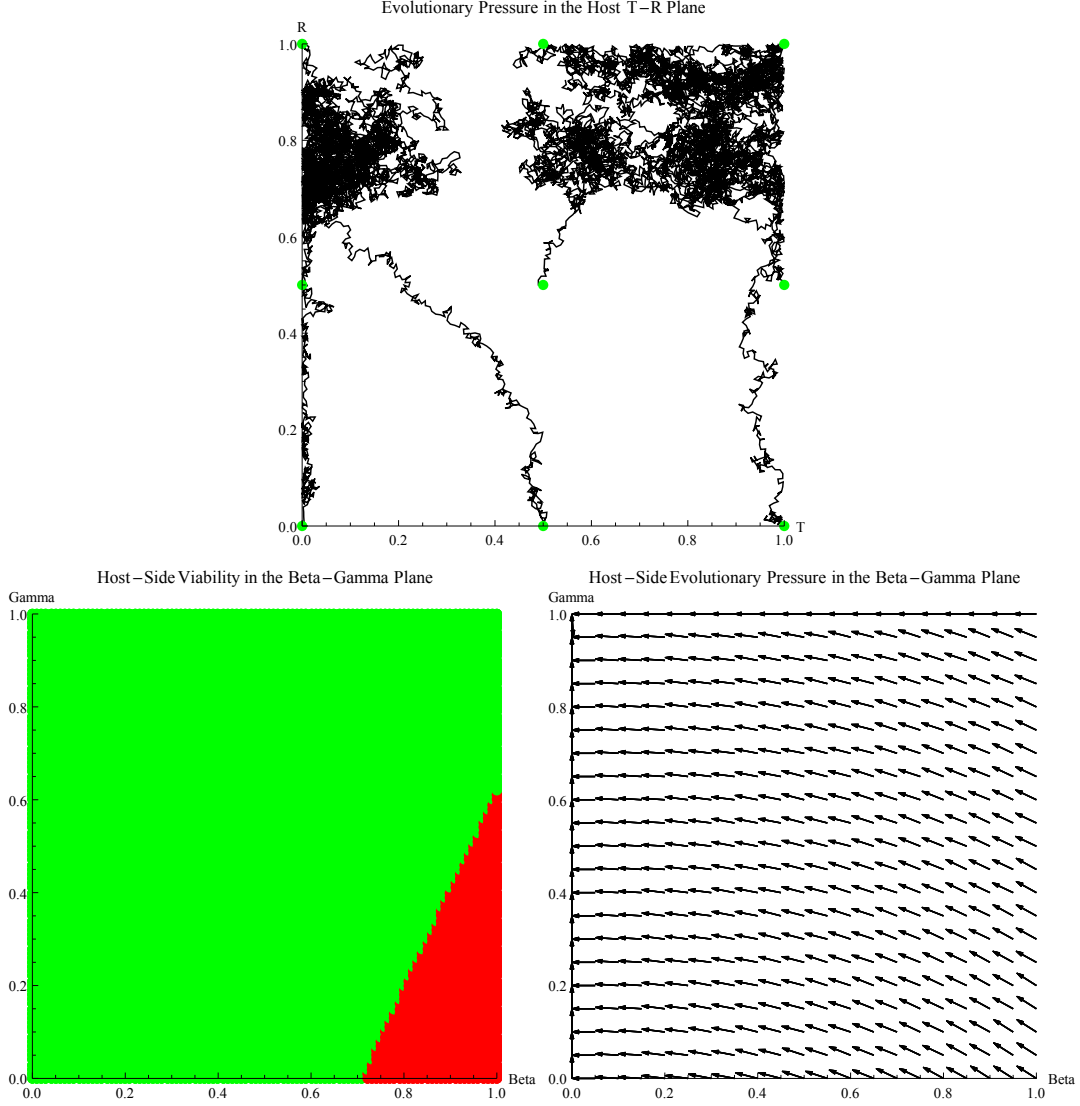


Figure 3.16: Left: This plot shows the result of simulations starting at  $(T, R) = (0.0, 0.0)$ ,  $(0.0, 0.5)$ ,  $(0.0, 1.0)$ ,  $(0.5, 0.0)$ ,  $(0.5, 0.5)$ ,  $(0.5, 1.0)$ ,  $(1.0, 0.0)$ ,  $(1.0, 0.5)$ ,  $(1.0, 1.0)$ , with 2000 time steps for each starting point. In this spatial simulation, the fixed parameters were  $G = 0.6$  and  $V = 0.35$ . Center: This plot shows the viable region (green) and nonviable region (red) of the host-side  $\beta$ - $\gamma$  plane. Right: The evolutionary pressure vector field computed from the ODE system.

### 3.10 Host $\beta$ - $\mu$ Evolution

For host-side  $\beta$ - $\mu$  evolution, we are uncertain about the direction for evolutionary pressure in  $\mu$  and expect evolutionary pressure to generally tend towards lower  $\beta$ , for reasons mentioned earlier. The simulation results for the host  $\beta$ - $\mu$  plane are shown in Figure 3.17.

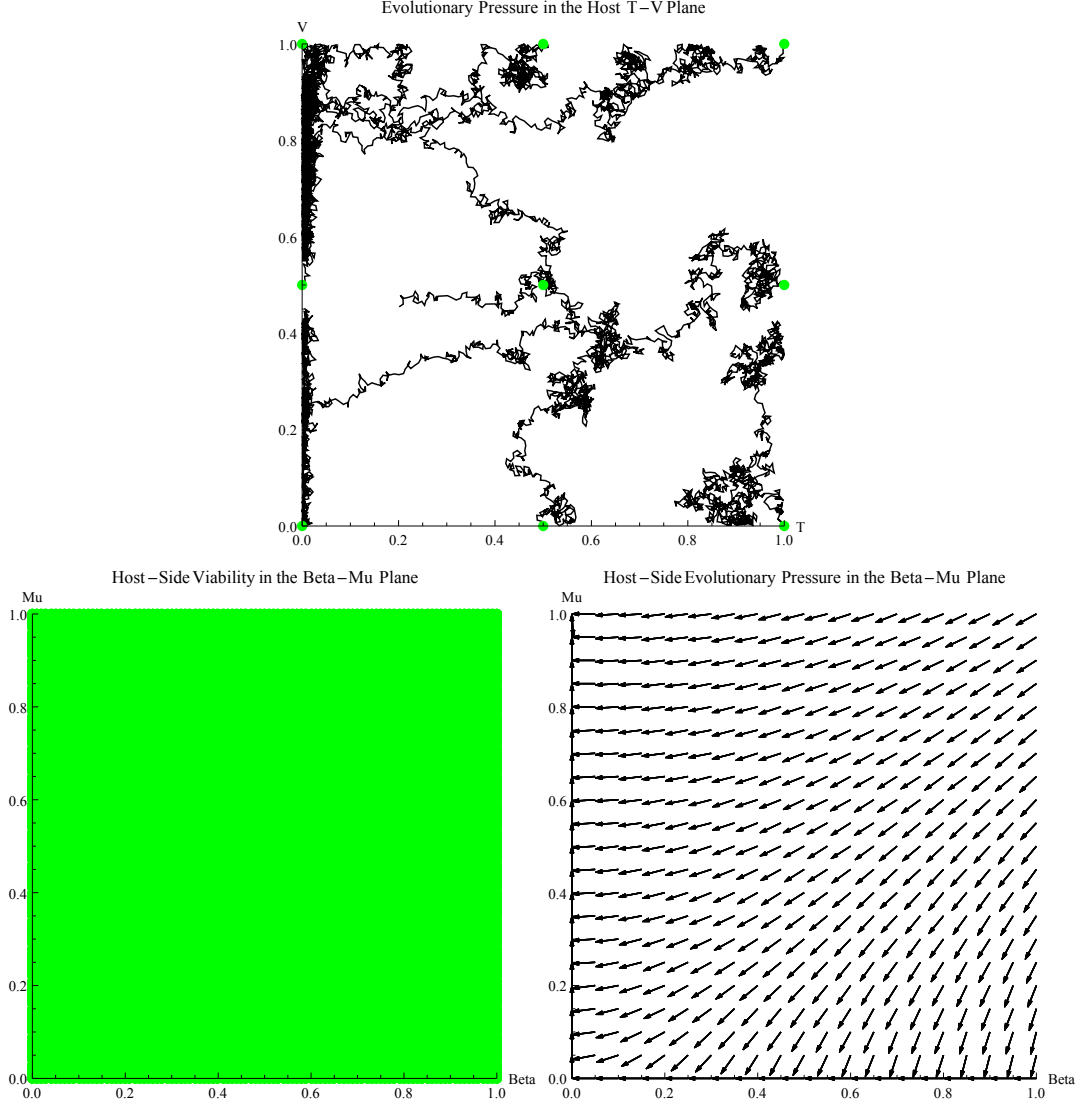


Figure 3.17: Left: This plot shows the result of simulations starting at  $(T, V) = (0.0, 0.0)$ ,  $(0.0, 0.5)$ ,  $(0.0, 1.0)$ ,  $(0.5, 0.0)$ ,  $(0.5, 0.5)$ ,  $(0.5, 1.0)$ ,  $(1.0, 0.0)$ ,  $(1.0, 0.5)$ ,  $(1.0, 1.0)$ , with 2000 time steps for each starting point. In this spatial simulation, the fixed parameters were  $G = 0.6$  and  $R = 0.1$ . Center: This plot shows the viable region (green) and nonviable region (red) of the host-side  $\beta$ - $\mu$  plane. Right: The evolutionary pressure vector field computed from the ODE system.

### 3.11 Host $\gamma$ - $\mu$ Evolution

For host-side  $\gamma$ - $\mu$  evolution, we are uncertain about the direction for evolutionary pressure in  $\mu$  and expect evolutionary pressure to generally tend towards higher  $\gamma$ , for reasons mentioned earlier. The simulation results for the host  $\gamma$ - $\mu$  plane are shown in Figure 3.18.

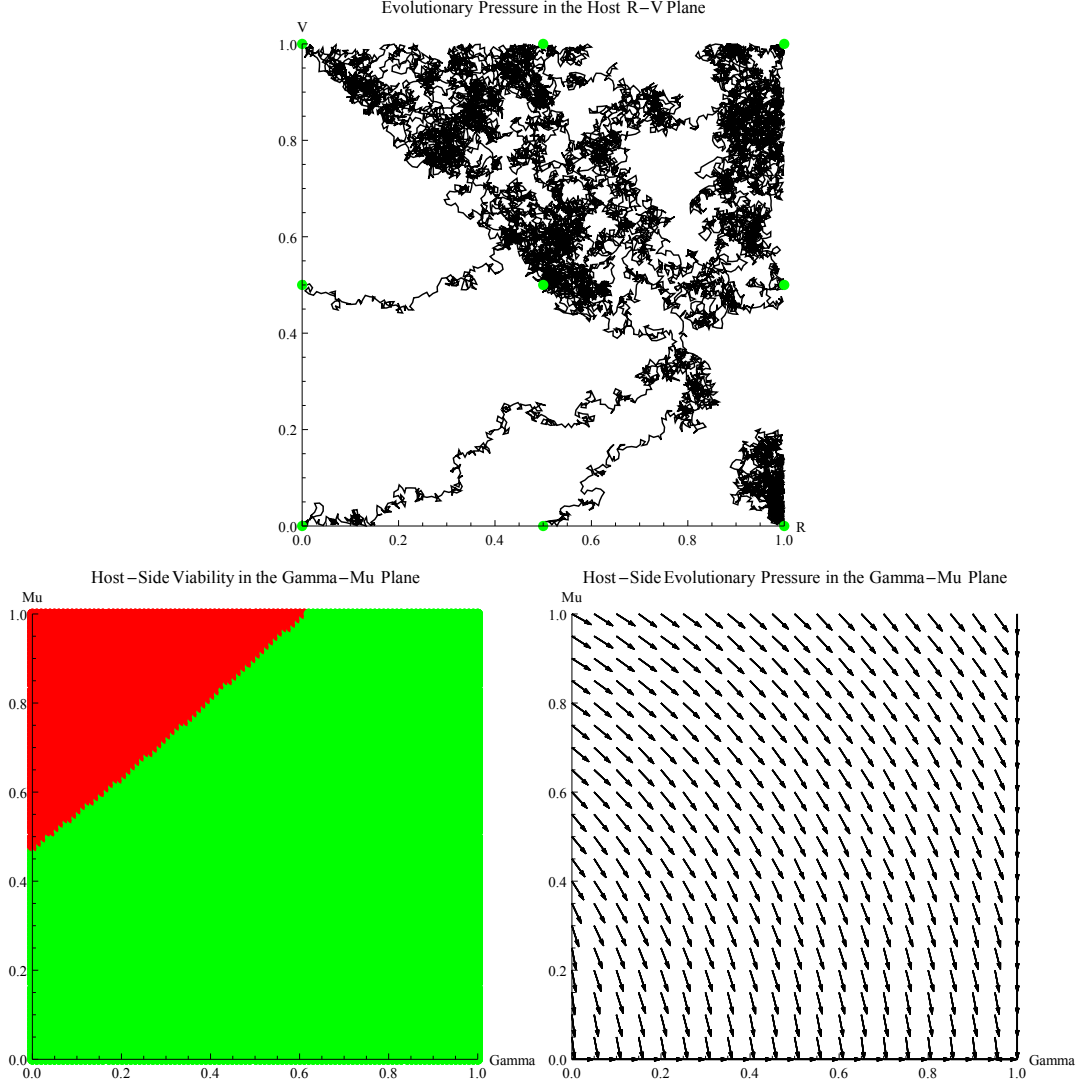


Figure 3.18: Left: This plot shows the result of simulations starting at  $(R, V) = (0.0, 0.0)$ ,  $(0.0, 0.5)$ ,  $(0.0, 1.0)$ ,  $(0.5, 0.0)$ ,  $(0.5, 0.5)$ ,  $(0.5, 1.0)$ ,  $(1.0, 0.0)$ ,  $(1.0, 0.5)$ ,  $(1.0, 1.0)$ , with 2000 time steps for each starting point. In this spatial simulation, the fixed parameters were  $G = 0.6$  and  $T = 0.7$ . Center: This plot shows the viable region (green) and nonviable region (red) of the host-side  $\gamma$ - $\mu$  plane. Right: The evolutionary pressure vector field computed from the ODE system.

# Chapter 4

## Discussion

Our results from individual-based spatial and mean-field differential equation models indicate that while the models are generally in qualitative agreement about the behavior of a host-pathogen system, several differences do exist.

### 4.1 Direction of Evolutionary Pressure

The ODE and spatial models generally agree on the broad direction of evolutionary pressure. For the same evolutionary plane, they agree on which parameters are increased by evolutionary pressure, and which ones are decreased. However, they sometimes differ on the precise direction of greatest evolutionary pressure. Further, our methods of constructing vector fields for the ODE system yield no information about magnitude of evolutionary pressure, so we are forced to infer it from the behavior of the spatial system.

#### 4.1.1 $\beta$ -Dependence of Parameters Associated with Infected Hosts

One interesting interaction between different host-side parameters is that as the value of  $\beta$  (transmissibility) decreases, the magnitude of evolutionary pressure for parameters associated with infected hosts,  $\gamma$  (recovery) and  $\mu$  (virulence), decreases as well. This is apparent in the subfigures on the right sides of Figures 3.16 and 3.17. We see that near the line where  $\beta = 0$ , the component of evolutionary pressure for the other parameter ( $\gamma$  or  $\mu$ ) is very small. The lines of evolutionary pressure are nearly horizontal (primarily  $\beta$  component)!

This implies that when  $\beta$  is low, the  $\gamma$  and  $\mu$  parameters become less important to the overall evolutionary trajectory of the system. This is simply a result of a decreased population of infected hosts. When  $\beta$  is low, fewer healthy hosts get infected. The infected proportion of the total host population is decreased. As a result, it becomes less important in determining the overall fate of the host population, and the  $\gamma$  and  $\mu$  parameters associated with it become less important as well.

## 4.2 Stochasticity in Spatial Model

While the basic differential equation model we studied is deterministic, the spatial model is clearly probabilistic. This has important consequences for the interpretation of our results. In a deterministic model, the results of a simulation will not change between trials. But in a probabilistic model, the outcome observed is only one element of a set of possibilities.

This general effect is particularly obvious in Figures 3.3 and 3.4. We see that while the deterministic ODE model predicts evolutionary trajectories in smooth paths shaped like part of the circumference of a circle, the spatial simulation yielded jagged lines in the same general direction. This is a consequence of the fact that in our spatial model, a species which is more fit can still be outcompeted by a less fit species, provided that it gets lucky.

### 4.2.1 As a Measure of Evolutionary Pressure

This general effect is most apparent when the magnitude of evolutionary pressure is low, and varying a parameter by a small amount produces a nearly negligible change in fitness. For example, we see this in Figure 3.8 along the T-axis. Once pathogens evolve to approximately zero recovery in the  $\gamma$ - $\beta$  plane, the only evolutionary pressure is in the positive  $\beta$  direction. Without a  $\gamma$  component, the overall evolutionary pressure is significantly reduced, and as a result we see large dark clumps around the T-axis, indicating that the species is spending a large number of time steps in that neighborhood, evolving slowly.

### 4.2.2 High Stochasticity in Non-Viable Region

Another interesting effect observed in Figures 3.13, 3.12, and others is that trajectories in the non-viable region of parameter space tend to evolve more slowly. We often see large clumps of footprints in that space, as one species has evolved haphazardly in that region, with a trajectory that looks almost like a unbiased random walk. This indicates that the bias — the evolutionary pressure — may be weaker in that region.

But why should evolutionary pressure be weaker in the non-viable region? In nature, harsher environments often correspond to stronger evolutionary pressure, forcing species to adapt more quickly or face extinction. One possible answer is in part an artifact of our implementation. Since we recognize that evolution still exists in the non-viable region of parameter space, we included non-viable species in our simulation and ignored the possibility of extinction. Since we defined greater fitness in the spatial model as simply a higher population after a given number of time steps, in the non-viable region we are actually choosing two non-viable species, and simply choosing the one that is becoming extinct at a slower rate.

But this increases the effects of stochasticity! If a species is increasing, then the effect of stochasticity on evolution decreases with time, since a higher population reduces the significance of random fluctuations. On the other hand, in the non-viable situation, the effects of stochasticity are increasing with time, making the evolution of the species more erratic and less likely to align with the true direction of evolutionary pressure.

So we see that this effect is not an actual decrease in evolutionary pressure brought on by non-viability. It is an apparent decrease in evolutionary pressure. The non-viable parameters

cause the species to suffer, and the population to decrease. This reduces the stochasticity-mitigating effect of having a large number of individuals. As a result, the actual direction of evolution becomes more weakly coupled to the direction of evolutionary pressure, and the evolutionary trajectory becomes unpredictable.

# Bibliography

- [1] Bayes, Thomas and Price, Richard, *An essay towards solving a problem in the doctrine of chances. by the late Rev. Mr. Bayes, FRS. Communicated by Mr. Price, in a letter to John Canton, AMFRS*, Philosophical Transactions (1683-1775) (1763), 370–418.
- [2] Levin, Simon A and Powell, Thomas M and Steele, JW, *Patch dynamics*, Tech. report, Springer-Verlag, New York, NY (United States), 1993.
- [3] Rand, DA and Keeling, M and Wilson, HB, *Invasion, stability and evolution to criticality in spatially extended, artificial host-pathogen ecologies*, Proceedings of the Royal Society of London. Series B: Biological Sciences **259** (1995), no. 1354, 55–63.
- [4] Frank, Steven A, *Models of parasite virulence*, Quarterly Review of Biology (1996), 37–78.
- [5] Gandon, Sylvain and Mackinnon, Margaret J and Nee, Sean and Read, Andrew F, *Imperfect vaccines and the evolution of pathogen virulence*, Nature **414** (2001), no. 6865, 751–756.
- [6] Okubo, Akira and Levin, Simon A, *Diffusion and Ecological Problems: Mathematical Models*, Springer, March 2002.
- [7] Galvani, Alison P, *Epidemiology meets evolutionary ecology*, Trends in Ecology & Evolution **18** (2003), no. 3, 132–139.